Fuel 235 (2019) 1052–1060

Contents lists available at ScienceDirect

Fuel

journal homepage: www.elsevier.com/locate/fuel

Full Length Article

Jet fuel density via GC × GC-FID

Petr Vozka[a], Brent A. Modereger[b], Anthony C. Park[c], Wan Tang Jeff Zhang[b], Rodney W. Trice[d], Hilkka I. Kenttämaa[b], Gozdem Kilaz[a,*]

[a] School of Engineering Technology, Fuel Laboratory of Renewable Energy (FLORE), Purdue University, West Lafayette 47907, IN, USA
[b] Department of Chemistry, Purdue University, West Lafayette 47907, IN, USA
[c] Agricultural & Biological Engineering, Purdue University, West Lafayette 47907, IN, USA
[d] School of Materials Engineering, Purdue University, West Lafayette 47907, IN, USA

ARTICLE INFO

Keywords:
Fuel density
GC × GC
Jet fuel
Alternative jet fuel
PLS
Weighted average
SVM

ABSTRACT

Aviation jet fuels contain over a thousand different hydrocarbons, making the prediction of their properties from chemical composition difficult. The density of a jet fuel at 15 °C is necessary for its certification. We present here an analytical approach for the determination of the density of jet fuels based on the chemical composition of the fuel determined via comprehensive two-dimensional gas chromatography with flame ionization detector (GC × GC-FID). The analysis was carried out using two-dimensional gas chromatography with electron ionization high-resolution time-of-flight mass spectrometry detection (GC × GC-TOF/MS) and flame ionization detection (GC × GC-FID). A detailed chemical composition analysis was performed on 50 samples, including petroleum-based aviation fuels and all approved alternative aviation fuel blending components. Fuel constituents were classified into seven hydrocarbon classes (*n*-paraffins, isoparaffins, monocycloparaffins, di- and tricycloparaffins, alkylbenzenes, cycloaromatic compounds, and alkylnaphthalenes) with the number of carbons in the range of 7–20. Several correlation algorithms and approaches were explored, including partial least squares regression (PLS) and support vector machines method (SVM), which yielded the most accurate results with mean absolute percentage errors of 0.1740% and 0.0984%, respectively. All used methods were validated utilizing uncalibrated validation samples.

1. Introduction

The density of (alternative) aviation fuels is one of the main parameters indicative of fuel quality. Fuel is filled into aircraft volumetrically; hence, density plays an especially important role in determining the total aircraft load as well as the aircraft range. Density is also used in flow calculations, fuel gauging, metering device adjustments, and fuel thermal expansion calculations [1].

Currently, five alternative aviation fuel blending components have been approved for use in gas turbine engines. These blending components are produced via several pathways: Fischer-Tropsch (FT) process using coal, natural gas, or biomass as feedstock [2]; hydroprocessing (hydrotreatment and hydroisomerization) of vegetable oils or animal fats [3]; sugar fermentation; and via an Alcohol-to-Jet (ATJ) process that is composed of three-steps (alcohol dehydration, oligomerization, and hydrogenation), utilizing corn, unrefined sugars, switchgrass, corn stover, corn fiber, glucose, wheat straw, liquefied corn starch, barley straw, sweet potato slurry, whey permeate, unrefined sugarcane, or woody biomass as a feedstock [4,5]. The chemical composition of the product obtained from each process is different, which requires attention as the constituents of these fuel blending components affect the fuel properties. These are expected to fall within a specific range as deemed necessary by fuel standards. One of the important properties for aviation fuels is the density at 15 °C. It is known that density increases in the order of paraffins < cycloparaffins < aromatics for the same carbon number. The density of *n*-paraffins is in most cases slightly higher than isoparaffins of the same carbon number. Establishing accurate fuel chemistry-property correlations is a still major subject of interest by multiple researchers.

The research focused on correlating the fuel chemical composition to its properties began in the 1980s [6–10]. First correlations between petroleum-based jet fuel composition and density were published in 1985 [10]. These studies used gas chromatography (GC), nuclear magnetic resonance (NMR) spectroscopy, and high-pressure liquid chromatography (HPLC) to determine the fuel chemical composition. Density predictions were based on the total content of *n*-paraffins and aromatic compounds. Later efforts focused on improving these models by adding distillation profile information into the calculations, which

* Corresponding author.
E-mail addresses: pvozka@purdue.edu (P. Vozka), gkilaz@purdue.edu (G. Kilaz).

https://doi.org/10.1016/j.fuel.2018.08.110
Received 8 July 2018; Received in revised form 18 August 2018; Accepted 24 August 2018
Available online 30 August 2018

allowed for the prediction of the density of alternative aviation fuels [7]. Alternative fuels used in these studies were obtained via hydroliquefaction and FT process of coal. Liu et al. [11] were the first to use an artificial neural network in 2007 to predict the density of aviation jet fuels based on their chemical composition determined via GC–MS. An alternative chemometric modeling (partial least squares) of near-infrared absorption spectra was first mentioned in the literature by Morris et al. [12]. This approach was later updated by utilizing GC–MS [13].

A comprehensive two-dimensional gas chromatography (GC × GC) capable of simultaneous mass spectrometry and flame ionization (FID) detection was used in 2017 for the development of quantitative chemical composition-property relationships for petroleum-based jet fuels and one FT synthetic fuel, as described by Shi et al. [14]. These authors tested several algorithms to correlate the density to fuel chemical composition. Partial least squares and modified weighted average methods yielded the most accurate results. However, these correlations were developed only for density values at 20 °C. Therefore, this study explores the use of different algorithms and approaches, which all potentially increase the predictive capability of the models studied. Additionally, this paper focuses on utilizing these methods to predict the density of aviation jet fuels at 15 °C, a capability pertinent to the field of aviation [15]. Furthermore, this is the first reported use of two-dimensional gas chromatography with a flame ionization detector (GC × GC-FID) for determining fuel density at 15 °C.

2. Experimental

2.1. Materials

Total sample set contained 50 samples composed of calibration and validation samples. Calibration sample set was comprised of 38 samples (Table 1), including 25 military petroleum-derived aviation jet fuels, 4 petroleum-derived Jet A fuels, 2 petroleum-derived Jet A-1 fuels, 6 synthetic or bio-derived alternative jet fuel blending components, and 1 jet fuel blend. Validation sample set was prepared manually by blending jet fuel and alternative aviation blending component from Table 1 in various ratios. Validation set contained 12 samples following the blending limitations of ASTM D7566: HEFA from tallow, HEFA from mixed fats, HEFA from camelina, and Fischer–Tropsch IPK were blended in 20 and 50 vol.% with Jet A. Alcohol-to-Jet was blended in 10 and 30 vol.% with Jet A. SIP Kerosene was blended in 5 and 10 vol.% with Jet A.

Table 1
List of tested samples.

Fuel	Composition	Note
aviation jet fuel[a]	25 different samples of F-24	petroleum-derived; military
aviation jet fuel	Jet A (ASTM)	petroleum-derived
aviation jet fuel[b]	Jet A (Chevron Pillips)	petroleum-derived
aviation jet fuel[b]	Jet A (Exxon Mobil)	petroleum-derived
aviation jet fuel[b]	Jet A (Shell)	petroleum-derived
av. blend component[b]	Alcohol-to-Jet (Gevo)	biofuel
av. blend component[b]	HEFA from tallow (UOP)	biofuel
av. blend component[b]	HEFA from mixed fats (Dynamic Fuels)	biofuel
av. blend component[b]	HEFA from camelina (UOP)	biofuel
av. blend component[b]	Fischer–Tropsch IPK (Sasol)	synthetic fuel
av. blend component[c]	SIP Kerosene (Amyris Bio.)	biofuel
aviation jet fuel	Jet A-1 (Twin Trans s.r.o.)	petroleum-derived
aviation jet fuel	Jet A-1 (Unipetrol, a.s.)	petroleum-derived
aviation jet blend[b]	50/50 vol.% Jet A/HEFA Camelina	

[a] Provided by the Naval Air Warfare Center Aircraft Division, Patuxent River, MD.
[b] Provided by the Wright-Patterson Air Force Base, Dayton, Ohio.
[c] Provided by the Aircraft Rescue and Firefighting division of Federal Aviation Administration, Egg Harbor Township, NJ.

In addition to above samples, density was measured for the following compounds: *n*-heptane (99% pure; Sigma-Aldrich), *n*-octane (≥99.5% pure; Sigma-Aldrich), *n*-nonane (≥95% pure; Fluka), *n*-decane (98% pure; ETI Science), *n*-dodecane (≥99% pure; Sigma-Aldrich), *n*-pentadecane (≥99% pure; Sigma-Aldrich), 2,2,4,4,6,8,8-heptamethylnonane (98% pure; Acros Organics), 1-ethyl-1-methylcyclohexane (> 99% pure; TCI), *n*-butylcyclohexane (≥99% pure, Sigma-Aldrich), decahydronaphthalene (≥99% pure; Fluka), toluene (99.8% pure, Acros Organics), 1,3-dimethylbenzene (99% pure; Alfa Aesar), 1,2,3,4-tetrahydronaphthalene (99% pure; Sigma-Aldrich), and 1-methylnaphthalene (97 + % pure; Acros Organics).

2.2. Density measurements

The density of all samples was measured using an SVM 3001 Stabinger Viscometer (Anton Paar) via ASTM D4052. The instrument was cleaned, calibrated, and checked for accuracy per instructions provided by the vendor. Anton Paar-certified standards (APN7.5 and APN26) were utilized. Samples were measured five times at 15 °C, and standard deviations were calculated automatically by the instrument. The average standard deviation value was −0.00003 g/cm^3, demonstrating a high precision for the measurements. Petroleum-based aviation fuel density value is required to be in the range between 0.775 and 0.840 g/cm^3 [15], while for alternative fuel blending components (ASTM D7566), the density value is required to be in the range of 0.730–0.770 g/cm^3 for Fischer-Tropsch Hydroprocessed Synthesized Paraffinic Kerosine, Synthesized Paraffinic Kerosine from Hydroprocessed Esters and Fatty Acids (HEFA), and Alcohol-to-Jet Synthetic Paraffinic Kerosene (ATJ), and between 0.765 and 0.780 g/cm^3 for Synthesized Iso-Paraffins from Hydroprocessed Fermented Sugars (SIP). Samples utilized in this study were selected to cover the complete density range.

2.3. Analysis of the chemical composition of the fuel samples

2.3.1. GC × GC-TOF/MS analysis

Qualitative analysis of the samples was performed using two-dimensional gas chromatography with electron ionization high-resolution time-of-flight mass spectrometry (GC × GC-TOF/MS). LECO Pegasus GC-HRT 4D (EI) High-Resolution TOF/MS (LECO Corporation, Saint Joseph, MI) was equipped with an Agilent 7890B gas chromatograph and a thermal modulator cooled with liquid nitrogen. The system was also equipped with an Agilent G4513A auto-injector. Primary mid-polar column Rxi-17Sil ms (60 m × 0.25 mm × 0.25 μm) was connected to a secondary nonpolar column Rxi-1 ms (2.0 m × 0.25 mm × 0.25 μm). Both columns were procured from Restek (Bellefonte, PA). The transfer line, ion source, and inlet temperatures were maintained at 300, 250, and 280 °C, respectively. Oven temperature program started at 40 °C (hold time 0.2 min) and ended at 160 °C (hold time 5 min) with a temperature ramp rate of 3 °C/min. The offsets in the temperature of the secondary oven and modulator were 15 and 15 °C, respectively. Modulation period was set to 1.2 s, with a hot pulse duration of 0.20 s. Each sample (10 μL) was diluted in 1 ml of *n*-hexane (≥99.0% pure; Acros Organics) in an autosampler vial (1:100 dilution). Injection volume was 0.5 μL with a 20:1 split ratio. Acquisition delay was 400 s. Ionization was achieved using 70 eV EI. The acquisition rate of mass spectra was 200 Hz with a detector gain voltage of 1750 V. ChromaTOF (Version 1.90.60.0.43266) was utilized for data collection (with an *m/z* of 45–550), processing, and analysis. Identification of the compounds was performed by matching the measured mass spectra (match threshold of > 700) with Wiley (2011) and NIST (2011) mass spectral databases.

2.3.2. GC × GC-FID analysis

For quantitative analysis, a comprehensive two-dimensional gas

chromatography (Agilent 7890B GC) with a flame ionization detector (FID) and a thermal modulator (LECO Corporation, Saint Joseph, MI) cooled with liquid nitrogen was used. This system was also equipped with an Agilent 7683B series injector and an HP 7683 series autosampler. Primary mid-polar column DB-17MS (30 m × 0.25 mm × 0.25 μm) was connected to a secondary nonpolar column DB-1MS (0.8 m × 0.25 mm × 0.25 μm). This column setup is known as a reversed phase setup and it allows for the improved separation of saturated and aromatic compounds. Both columns were provided by Agilent (Santa Clara, CA). FID and inlet temperatures were 300 and 280 °C, respectively. Oven temperature program started at 40 °C (hold time 0.2 min) and ended at 160 °C (hold time 5 min) with a temperature ramp rate of 1 °C/min. Secondary oven and modulator temperature offsets were 55 and 15 °C, respectively. Modulation period was set to 6 s with a hot pulse duration of 1.06 s. Each sample (10 μL) was diluted in 1 ml of dichloromethane (99.9% pure; Acros Organics) in an autosampler vial (1:100 dilution). Injection volume was 0.5 μL with a 20:1 split ratio. Acquisition delay was 165 s. FID data were collected at an acquisition rate of 200 Hz. GC × GC-FID classification utilizing ChromaTOF software (version 4.71.0.0 optimized for GC × GC-FID) has been described in detail in a previous publication [16]. Fig. 1 displays the fuel constituent classification established in this study. Classification is based on seven hydrocarbon classes (*n*-paraffins, isoparaffins, monocycloparaffins, di- and tricycloparaffins, alkylbenzenes, cycloaromatic compounds (indans, tetralins, indenes, etc.), and alkylnaphthalenes) with 7–20 carbon atoms. The weight percentage of each compound in the sample was calculated by utilizing the ratio of the compound peak area to the sum of all peak areas measured for the sample.

2.3.3. Chemical composition-density correlation algorithms

Three statistical modeling methods were used in order to process the compound weight percent data obtained from GC × GC-FID: weighted average (WA) method, partial least squares (PLS) regression, and a high dimensional method using regularized support vector machines (SVM).

WA has been described in a previous paper where middle distillates were studied [16]. Briefly, the density of the sample can be determined by calculating the sum of the density of each compound group weighted by the weight percentage of each group as expressed in Eq. (1).

$$D_{(g/cm^3)} = \sum_{i=1}^{7} \sum_{j=1}^{21} (a_{i,j} b_{i,j}) \tag{1}$$

where a is the density (Table 3) and b is the weight fraction. The subscripts i and j refer to the hydrocarbon class and number of carbon atoms, respectively.

PLS is a common methodology in linear multivariate regression. This method is commonly used in chemometrics. It is derived from principal component regression and acts as its "successor". PLS avoids the errors in a linear regression that occur in cases where the input data matrix X is not full rank (more predictors than observations or more observations than predictors). This is avoided by creating a lower dimensional projection in order to capture linear correlations and variability, which is the foundation of principal component analysis. This still does not encompass the relevance of principal components that may influence the response variable at different levels. To fix this problem, PLS incorporates collinearities between input matrix X and response matrix Y. The general underlying model is as follows: let X be an n x p matrix of predictor variables and Y be an n x q matrix of response variables. The response matrix can then be approximated as stated in Eq. (2).

$$Y = y_0 + T_A Q_A^T + F_A \tag{2}$$

This can be rewritten via the substitution of variables into Eq. (3)

$$Y = b_{0A} + XB_A + F_A \tag{3}$$

where $B_A = V_A Q_A^T$, $b_{0A} = y_0 - x_0 B_A$, and F_A is the vector of residuals. The vector of residuals and intercepts can be added together into one intercept value. Here, Q_A is the coupling between individual variables in Y and the A orthogonal components in the matrix $T_A = (X - x_0)V_A$. T_A can be thought of as scaled scores which define the covariance of the rows of X. What differentiates PLS from a principal component

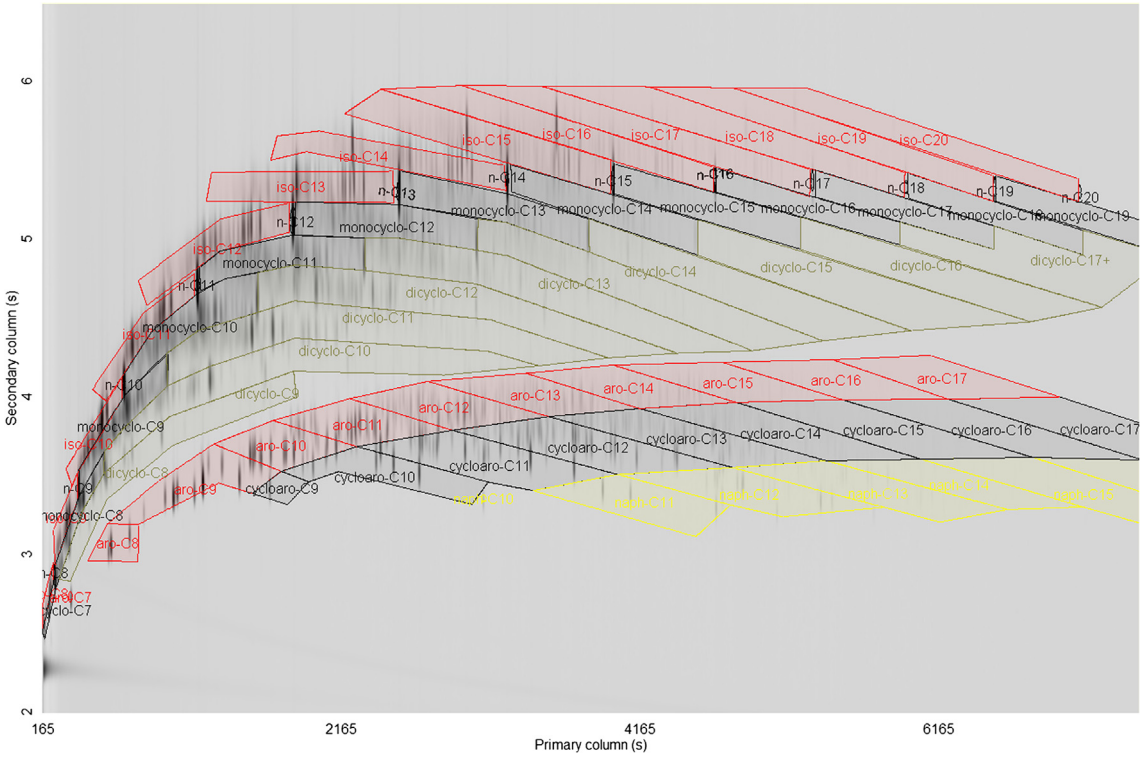

Fig. 1. F-24 (Luke AFB, AZ) GC × GC-FID chromatogram showing classification regions used.

Table 2
The chemical compositions (wt%) of SIP Kerosene (Amyris Bio.), HEFA from camelina (UOP), Jet A-1 (Unipetrol, a.s.), and F-24 (Luke AFB, AZ) obtained by using GC × GC-FID.

n-paraffins	SIP	HEFA	Jet A-1	F-24
C8	0.00	1.56	0.79	0.28
C9	0.00	2.15	1.45	2.61
C10	0.00	1.38	4.66	3.30
C11	0.00	0.96	6.81	3.22
C12	0.00	0.83	5.59	2.63
C13	0.00	0.65	3.50	2.27
C14	0.00	0.25	0.58	1.72
C15	0.00	0.51	0.04	1.18
C16	0.00	0.13	0.00	0.68
C17	0.00	0.10	0.00	0.27
C18	0.00	0.00	0.00	0.11
C19	0.00	0.00	0.00	0.04
C20	0.00	0.00	0.00	0.01
total *n*-paraffins	0.00	8.53	23.41	18.32
isoparaffins	SIP	HEFA	Jet A-1	F-24
C8	0.00	1.48	0.48	0.41
C9	0.00	11.18	1.57	2.60
C10	0.00	11.36	3.48	5.39
C11	0.00	9.88	7.12	4.91
C12	0.00	8.48	6.07	4.18
C13	0.00	8.17	5.86	4.41
C14	0.05	6.29	2.57	3.35
C15	99.43	5.59	0.32	2.84
C16	0.03	2.35	0.03	1.70
C17	0.00	21.26	0.00	0.87
C18	0.00	3.66	0.00	0.49
C19	0.00	0.00	0.00	0.21
C20	0.00	0.00	0.00	0.05
total isoparaffins	99.52	89.71	27.50	31.39
monocycloparaffins	SIP	HEFA	Jet A-1	F-24
C8	0.00	0.81	2.03	3.48
C9	0.00	0.51	4.00	4.09
C10	0.00	0.29	6.88	4.58
C11	0.00	0.08	4.97	3.71
C12	0.00	0.03	3.86	3.65
C13	0.00	0.00	0.83	2.74
C14	0.42	0.00	0.00	1.79
C15	0.00	0.00	0.00	0.97
C16	0.00	0.00	0.00	0.35
C17	0.00	0.00	0.00	0.03
C18	0.00	0.00	0.00	0.00
C19+	0.00	0.00	0.00	0.00
total monocycloparaffins	0.42	1.73	22.58	25.38
di- and tricycloparaffins	SIP	HEFA	Jet A-1	F-24
C8	0.00	0.00	0.22	0.30
C9	0.00	0.00	1.13	0.95
C10	0.00	0.00	1.80	1.44
C11	0.00	0.00	1.61	1.54
C12	0.00	0.00	0.99	1.42
C13	0.00	0.00	0.08	0.60
C14	0.00	0.00	0.00	0.33
C15	0.00	0.00	0.00	0.10
C16	0.00	0.00	0.00	0.00
C17+	0.00	0.00	0.00	0.00
total di- and tricycloparaffins	0.00	0.00	5.82	6.68
total cycloparaffins	0.42	1.73	28.40	32.06
alkylbenzenes	SIP	HEFA	Jet A-1	F-24
C8	0.00	0.01	1.27	1.30
C9	0.00	0.02	4.83	3.16
C10	0.00	0.00	4.30	3.42
C11	0.00	0.00	2.45	1.76
C12	0.00	0.00	1.23	1.43
C13	0.00	0.00	0.42	0.89
C14	0.00	0.00	0.01	0.40
C15	0.06	0.00	0.00	0.26

Table 2 (*continued*)

alkylbenzenes	SIP	HEFA	Jet A-1	F-24
C16	0.00	0.00	0.00	0.13
C17+	0.00	0.00	0.00	0.02
total alkylbenzenes	0.06	0.03	14.51	12.78
cycloaromatic compounds	SIP	HEFA	Jet A-1	F-24
C9	0.00	0.00	0.21	0.07
C10	0.00	0.00	0.98	0.45
C11	0.00	0.00	2.43	1.24
C12	0.00	0.00	1.30	1.14
C13	0.00	0.00	0.17	0.75
C14	0.00	0.00	0.00	0.40
C15	0.00	0.00	0.00	0.21
C16	0.00	0.00	0.00	0.01
C17+	0.00	0.00	0.00	0.00
total cycloaromatic compounds	0.00	0.00	5.10	4.27
alkylnaphthalenes	SIP	HEFA	Jet A-1	F-24
C10	0.00	0.00	0.21	0.07
C11	0.00	0.00	0.76	0.30
C12	0.00	0.00	0.11	0.42
C13	0.00	0.00	0.00	0.26
C14	0.00	0.00	0.00	0.09
C15	0.00	0.00	0.00	0.04
C16+	0.00	0.00	0.00	0.00
total alkylnaphthalenes	0.00	0.00	1.08	1.18
total aromatic compounds	0.06	0.03	20.69	18.23

regression method is the definition of V_A. While this term refers to the maximal covariance in X, the term references the maximal covariance between X and Y in PLS. When considering each hydrocarbon class as a single predictor, PLS is a very powerful tool with great predictive capabilities. However, in very highly underdetermined systems, PLS may not perform as effectively. Despite this, PLS is capable of compensating for these systems to some extent [17–19].

The final model relies heavily on Support Vector Machines (SVM). The philosophy behind SVM is to apply a machine learning method onto creating a linear regression model [20]. This model can be derived by applying a least squares regression formula on a derived SVM model, Eq. (4).

$$y(x) = \sum_{k=1}^{N} a_k K(x, x_k) + b \tag{4}$$

which is then considered given a training set $\{x_k, y_k\}_{k=1}^{N}$. Consecutively, these parameters can be estimated using stochastic gradient descent (SGD) or dual coordinate descent (DCD) method. While both can be used for large scale optimization of the SVM model, the SGD method depends on a stochastic factor z_i added to a gradient descent method expressed in Eq. (5).

$$w_{t+1} = w_t - \gamma_t \nabla_w Q(z_t, w_t) \tag{5}$$

In spite of the fact that the above model is a drastic simplification of the gradient descent method, this results in an approximation of the true gradient that can include a lot of noise [21]. Alternatively, the DCD method is a newer method, which can more efficiently solve linear SVM methods [22,23]. Both methods were observed to be suitable for cases with underdetermined systems, which is useful in creating a predictive model that accounts for each compound.

3. Results and discussion

3.1. GC × GC qualitative analysis

When calculating the density of a group of compounds two approaches can be used. An average density can be calculated by considering the density of every compound of a particular hydrocarbon class and carbon number. However, this process can become very

cumbersome as the number of isomers in a given compound group increases. For example, finding the density of *n*-paraffin with eight carbons involves finding the density of only a single compound: *n*-octane. However, determining the average density of all alkylbenzenes with eight carbons requires involving five isomers (ethylbenzene, 1,1-dimethylbezene, 1,2-dimethylbezene, 1,3-dimethylbezene, and 1,4-dimethylbezene). The number of structural isomers (not including enantiomers) for dodecane, tridecane, and tetradecane are 355, 802, and 1858, respectively. The complexity of this approach is avoided by using the second approach, which is based on a singular compound used to represent each hydrocarbon class and carbon number. Therefore, the GC × GC-TOF/MS chromatograms were studied for all 38 samples. After considering only those peaks with a minimum similarity score of 700 and excluding any peaks that were identified as the same compound (except that with the greatest peak area), a total of 10,667 peaks were detected with peak area percent over 0.000672%. The representative compound was selected as the compound with the greatest peak area percent for each compound class, only if the density for that compound could be found in the literature. The approach for the cases where density was not found is explained in Section 3.3.

3.2. GC × GC quantitative analysis

The standards utilized for the determination of the linear range of the signal obtained using the GC × GC instrument were *n*-nonane and naphthalene with concentration values in the range of 1–500 ppm. The regression coefficient (R^2) values of 0.9999 and 0.9998 for *n*-nonane and naphthalene, respectively, validated linearity. Reliability of the GC × GC method was validated by comparing the results to those from three US military research labs. A sample chromatogram of the set of experiments is displayed in Fig. 1. Table 2 provides the comparative data obtained for the four samples representing different fuel types.

Petroleum-derived jet fuels contain approximately 2000 hydrocarbon compounds. For the purpose of classification, these compounds were divided into pertinent groups based on their hydrocarbon classes and carbon number (GC × GC-FID classification). After this division, depending on the number of possible isomers, each compound group contained one (*n*-paraffins, naphthalene, etc.) or several compounds. Jet fuels can also contain trace amounts (ppm) of heteroatoms (S, N, O), which are strictly limited for aviation jet fuels (ASTM D1655) and aviation jet fuel blending components (ASTM D7566). Therefore, the classification did not take heteroatoms into consideration.

3.3. WA method

Stemming from the fact that volume is an additive property for hydrocarbon mixtures, it is reasonable to assume that density is also an additive property. Thus, the WA method can be considered as an effective approach for fuel (hydrocarbon mixture) density calculations. In order to utilize the WA method for correlation of the chemical composition and density, a representative compound was selected for groups that contained more than one compound, as discussed above. In some cases, (C18- and C19-isoparaffins, C16- and C18-monocycloparaffins, and C15-alkylnaphthalenes), the density of representative compounds could not be found in the literature. For these compound groups, a different representative compound was chosen for which the density could be found in the literature. New representative compounds were chosen to have only methyl- alkyl groups for isoparaffins; and only a single alkyl chain for monocycloparaffins and alkylnaphthalenes. Representative compounds and their measured or estimated densities obtained from the literature are shown in Table 3. The density values of these compounds were subsequently used in the calculations. Utilizing the 14 values measured here and the 55 values found in literature, a density matrix was composed. It should be noted that if density values at 15 °C were not available in the literature, values at two separate temperatures were utilized to intra- or extrapolate, assuming a linear relationship between density and temperature in that temperature range. Density values taken from the literature for temperatures different from 15 °C can be found in Supplemental material (Table S1). In cases where none of the above steps were possible, the representative compound was assigned to be the one having the next greatest peak area percentage (quotient of peak area and a total peak area of chromatogram).

Above approach is different from the one published previously [14], where the authors used the average density of the most abundant compounds in each group. The advantage of the current method (representative compound as opposed to density average) lies in the fact that all compounds in a given class have similar densities [14]. Therefore, using the density values of compounds with the greatest peak area percent offers a simpler and faster approach. Additionally, this method has the potential to produce more accurate results than using the average density values of some compounds within the group.

Fig. 2 depicts a plot of measured density versus density obtained using GC × GC-FID and the WA method. In general, the WA method predicted slightly lower density values than the empirical values. Both data sets (calibration and validation) were measured. In this case, the validation set served rather expand the total sample set than validation. However, all data points were within a range of ± 2% relative error. The mean absolute percentage error (MAPE) was 0.6855% and the correlation coefficient (R^2) was 0.9327. The repeatability and reproducibility of ASTM D4052 are 0.00045–0.00031 and 0.0019–0.0344 g/cm^3, respectively. Therefore, the WA method gave some results with relative errors that were higher than the repeatability and/or reproducibility of ASTM D4052. Therefore, utilizing a more effective algorithm has the potential to decrease the error observed for the WA method.

3.4. PLS and SVM method

In this study, composition matrix refers to the matrix of weight fraction data generated by GC × GC-FID. The algorithms utilized the composition matrix in one of two ways: (i) weight fractions of each carbon number in per hydrocarbon class were summed and used as a predictor; seven predictors total, or (ii) the weight fraction of each compound in the compositional matrix was used; 98 predictors in total. Density matrix is the matrix of density values of the representative compounds for each group. The product matrix is the result of an elementwise multiplication of composition and density matrices. The product matrix was used in the same way as the composition matrix to improve the predictive capabilities of the model.

PLS and SVM methods were applied to the compositional matrix as well as the product matrix. When using 98 predictors, 25 predictors were disregarded due to one of three reasons: (i) compound of that compound group does not exist (e.g., C8-alkylnaphthalenes), (ii) no members of that compound group were detected in any fuel samples, or (iii) the model placed insignificant weight on the predictor. For the product matrix, 30 predictors were disregarded for the same reasons.

A disadvantage to the approach described above is the underdetermination of the predictor matrix. However, PLS method can prevent the overfitting problem that occurs with an underdetermined system through maximizing covariance. Unlike PLS, SVM is capable of regulating the data during the “learning” procedure. This is an alternative way to prevent overfitting. In order to prevent overfitting for the underdetermined case, the ridge method (Tikhonov regularization) was used for regulation.

Table 4 shows the model coefficients of different composition-density correlations for the approach with seven predictors. In Table 4, the first coefficient stands for intercept, while the other coefficients correspond to the sum of each hydrocarbon class in the order aforementioned. The coefficients for the approach with 98 predictors can be found in Supplementary material (Table S2). Eq. (6) was used for calculating density by using seven predictors (n = 7) or 98 predictors

Table 3
Selected compounds and their density values at 15 °C. A single citation represents density found in literature at 15 °C, two citations represent density estimated from two density values found in the literature, and no citation represents density determined experimentally in this work.

compound	Hydrocarbon class[a]	Carbon number	density (g/cm^3)
n-heptane	A	7	0.6884
n-octane	A	8	0.7072
n-nonane	A	9	0.7221
n-decane	A	10	0.7341
n-undecane	A	11	0.7443/[24]
n-dodecane	A	12	0.7528
n-tridecane	A	13	0.7601/[25,25]
n-tetradecane	A	14	0.7669/[26,27]
n-pentadecane	A	15	0.7726
n-hexadecane	A	16	0.7768/[28,28]
n-heptadecane	A	17	0.7815/[29,29]
n-octadecane	A	18	0.7852/[29,30]
n-nonadecane	A	19	0.7889/[29,29]
3,3-dimethylpentane	B	7	0.6973/[31,32]
2,4-dimethylhexane	B	8	0.7083/[33]
4-ethyl-2-methylhexane	B	9	0.7270/[29,29]
2-methylnonane	B	10	0.7247/[34,35]
2-methyldecane	B	11	0.7407/[36,36]
2,2,4,6,6-pentamethylheptane	B	12	0.7508/[37,38]
3-methyldodecane	B	13	0.7618/[36,36]
3-methyltridecane	B	14	0.7685/[36,36]
2,6,10-trimethyldodecane	B	15	0.7810/[39,40]
2,2,4,4,6,8,8-heptamethylnonane	B	16	0.7881
4-methylhexadecane	B	17	0.7824/[36,36]
2-methylheptadecane	B	18	0.7837/[36,36]
2,6,10,14-tetramethylpentadecane	B	19	0.7865/[41,42]
ethylcyclopentane	C	7	0.7708/[43,43]
ethylcyclohexane	C	8	0.7923/[44,44]
1-ethyl-1-methylcyclohexane	C	9	0.8063
butylcyclohexane	C	10	0.8032
pentylcyclohexane	C	11	0.8086/[29,45]
hexylcyclohexane	C	12	0.8118/[46,46]
heptylcyclohexane	C	13	0.8144/[29,29]
octylcyclohexane	C	14	0.8172/[29,29]
1-(1,5-dimethylhexyl)-4-methylcyclohexane	C	15	0.8280/[47]
decylcyclohexane	C	16	0.8220/[48,48]
undecylcyclohexane	C	17	0.8240/[29,29]
dodecylcyclohexane	C	18	0.8256/[29,29]
octahydropentalene	D	8	0.8702/[49,50]
octahydro-1H-Indene, cis-	D	9	0.8839/[49,51]
decahydronaphthalene	D	10	0.8734
2-*syn*-methyl-*cis*-decalin	D	11	0.8823/[52,53]
2-ethyldecahydronaphthalene	D	12	0.8842/[53,53]
2-methyl-1,1′-bicyclohexyl, cis-	D	13	0.8881/[53,54]
1-(cyclohexylmethyl)-2-methylcyclohexane, trans-	D	14	0.8879/[53,55]
decahydro-1,6-dimethyl-4-(1-methylethyl)naphthalene	D	15	0.8883/[56]
1,1′-(1-methyl-1,3-propanediyl)bis-cyclohexane	D	16	0.8833/[57,57]
toluene	E	7	0.8715
1,3-dimethylbenzene	E	8	0.8685
1,2,3-trimethylbenzene	E	9	0.8984/[58,58]
1,2,3,4-tetramethylbenzene	E	10	0.9077/[59,60]
1-*sec*-butyl-4-methylbenzene	E	11	0.8700/[29,29]
hexylbenzene	E	12	0.8615/[28,28]
heptylbenzene	E	13	0.8604/[29,29]
octylbenzene	E	14	0.8599/[61]
1-(1,5-dimethylhexyl)-4-methylbenzene	E	15	0.8524/[47]
indane	F	9	0.9680/[62,62]
1,2,3,4-tetrahydronaphthalene	F	10	0.9727
2,3-dihydro-1,6-dimethyl-1H-indene	F	11	0.9313/[63,63]
1,2,3,4-tetrahydro-5,7-dimethylnaphthalene	F	12	0.9629/[29,29]
1,2,3,4-tetrahydro-1,1,6-trimethylnaphthalene	F	13	0.9362/[64,65]
6-(1,1-dimethylethyl)-1,2,3,4-tetrahydronaphthalene	F	14	0.9463/[66]
6-(1-ethylpropyl)-1,2,3,4-tetrahydronaphthalene	F	15	0.9321/[67,67]
naphthalene	G	10	1.0168/[68,68]
1-methylnaphthalene	G	11	1.0278
1,7-dimethylnaphthalene	G	12	1.0060/[29,29]
1-propylnaphthalene	G	13	0.9916/[29,69]
1-methyl-7-(1-methylethyl)naphthalene	G	14	0.9797/[70]
pentylnaphthalene	G	15	0.9716/[71,29]

[a] A – *n*-paraffins, B – isoparaffins, C – monocycloparaffins, D – di- and tricycloparaffins, E – alkylbenzenes, F – cycloaromatic compounds, and G – alkylnaphthalenes.

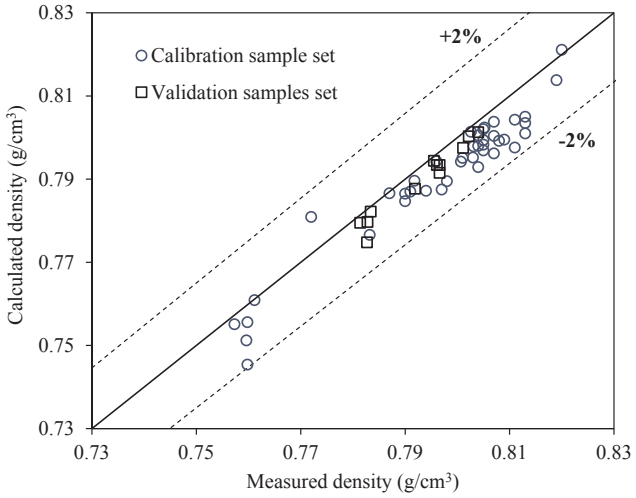

Fig. 2. Measured density versus density obtained using GC × GC-FID data and the WA method.

Table 4
Correlation coefficients for PLS and SVM using seven predictors.

Correlation	Coefficients
PLS *product*	β_0 = 0.38293, β_a = [0.00470, 0.00500, 0.00596, 0.00508, 0.00519, 0.00614, 0.00637]
PLS *composition*	β_0 = 1.55109, β_a = [−0.00831, −0.00788, −0.00683, −0.00722, −0.00711, −0.00573, −0.00504]
SVM *product*	β_0 = 0.40919, β_a = [0.00423, 0.00466, 0.00582, 0.00451, 0.00512, 0.00533, 0.00574]
SVM *composition*	β_0 = 0, β_a = [0.00727, 0.00760, 0.00885, 0.00797, 0.00836, 0.00936, 0.00951]

(n = 98). Table 5 presents a comparison of the results obtained using each correlation and the product matrix (*product*) or the composition matrix (*composition*) for calibration and validation set. The PLS method predicted the density values of aviation jet fuels (at 15 °C) with the lowest mean absolute percentage error and the highest R^2 value when seven predictors were used. However, the SVM method predicted the density values of jet fuels most accurately when 98 predictors were used. The product matrix improved the results for both models. Figs. 3 and 4 display plots of measured density values versus density values derived from GC × GC-FID data output utilizing PLS and SVM methods for both calibration and validation sets, respectively.

$$\rho = \beta_0 + \left(\sum_{a=1}^{n} \beta_a W_a\right) \quad (6)$$

where β_0 is the intercept, β_a is the coefficient of the compound group *a*, and W_a is the wt% of the compound group *a*.

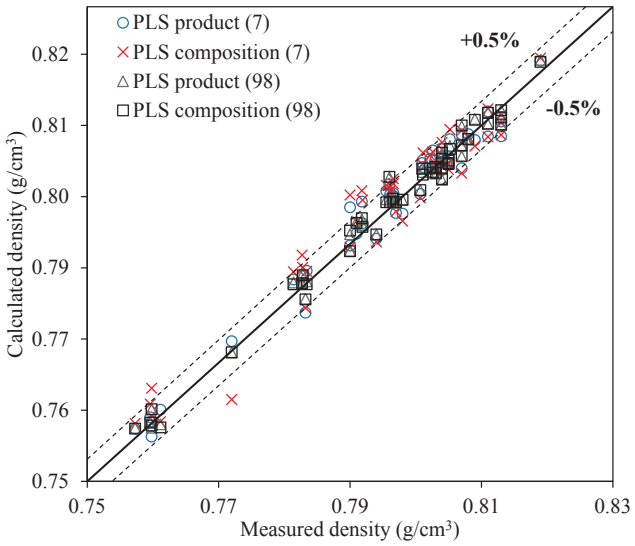

Fig. 3. Measured density versus density derived from GC × GC-FID data and the PLS method.

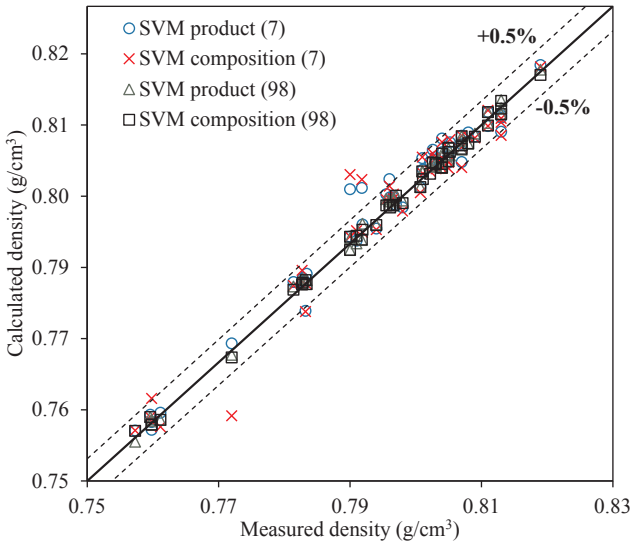

Fig. 4. Measured density versus density derived from GC × GC-FID data and the SVM method.

4. Conclusions

In this study, a method for the determination of density from chemical compositions determined via two-dimensional gas chromatography with FID was developed for aviation fuels and alternative fuel

Table 5
Comparison of mean absolute percentage errors (MAPE) and correlation coefficients (R^2).

Correlation	Calibration set		Validation set		Total set	
	MAPE (%)	R^2	MAPE (%)	R^2	MAPE (%)	R^2
PLS *product* (7)	0.2575	0.9769	0.2508	0.9938	0.2559	0.9746
PLS *composition* (7)	0.3493	0.9584	0.4884	0.9842	0.3827	0.9459
SVM *product* (7)	0.2425	0.9742	0.1970	0.9964	0.2315	0.9744
SVM *composition* (7)	0.3231	0.9530	0.1304	0.9873	0.2769	0.9546
WA (98)	0.7672	0.9330	0.4064	0.9536	0.6855	0.9327
PLS *product* (98)	0.1914	0.9879	0.1621	0.9947	0.1844	0.9869
PLS *composition* (98)	0.1912	0.9877	0.1193	0.9940	0.1740	0.9874
SVM *product* (98)	0.1068	0.9970	0.1299	0.9972	0.1124	0.9961
SVM *composition* (98)	0.1130	0.9967	0.0522	0.9976	0.0984	0.9967

blending components. This work focused on density values at 15 °C, which is a standard in the aviation industry. Three correlation algorithms were explored: the weighted average method (WA), partial least squares regression (PLS), and a high dimensional algorithm using regulated support vector machines method (SVM). Density results derived this way were compared to those obtained empirically from a Stabinger Viscometer via ASTM. When using the summed wt% of each hydrocarbon class, the SVM method yielded the most accurate prediction with a mean absolute percentage error (MAPE) of 0.2315%. Alternatively, when 98 predictors were used, the SVM method was observed to yield the most accurate results with a MAPE of 0.0984%. Additionally, use of the product matrix improved the results for both models. Moreover, these methods were validated utilizing uncalibrated validation samples. This work can be expanded to additional fuel properties that will enable the manufacturing of alternative aviation fuels with the specific chemical composition.

Acknowledgements

This work was supported by the US Navy, Office of Naval Research through Grant N000141613109 awarded by the Naval Enterprise Partnership Teaming with Universities for National Excellence (NEPTUNE) Center for Power and Energy Research. Our special thanks extend to Dr. Richard Carlin, Dr. Maria Medeiros, Richard Kamin, Dr. Michael Peretich, and Dr. Thomas N. Loegel.

Appendix A. Supplementary data

Supplementary data associated with this article can be found, in the online version, at https://doi.org/10.1016/j.fuel.2018.08.110.

References

[1] Coordinating Research Council. Handbook of Aviation Fuel Properties. Defense Technical Information Center; 1983.
[2] De Klerk A. Fischer-Tropsch Jet Fuel Process. Google Patents; 2014.
[3] Gupta KK, Rehman A, Sarviya RM. Bio-fuels for the gas turbine: a review. Renewable Sustainable Energy Rev 2010;14(9):2946–55.
[4] Wang WC, Tao L. Bio-jet fuel conversion technologies. Renewable Sustainable Energy Rev 2016;53:801–22.
[5] Alcohol To Jet (ATJ) emerging through ASTM, in ICAO aviation and sustainable alternative fuels workshop. 2011, BYOGY Renewables: Montreal, Canada.
[6] Cookson DJ, Smith BE. Calculation of jet and diesel fuel properties using carbon-13 NMR spectroscopy. Energy Fuels 1990;4(2):152–6.
[7] Cookson DJ, Iliopoulos P, Smith BE. Composition-property relations for jet and diesel fuels of variable boiling range. Fuel 1995;74(1):70–8.
[8] Cookson DJ, Lloyd CP, Smith BE. Investigation of the chemical basis of kerosene (jet fuel) specification properties. Energy Fuels 1987;1(5):438–47.
[9] Cookson DJ, Smith BE. Observed and predicted properties of jet and diesel fuels formulated from coal liquefaction and Fischer-Tropsch feedstocks. Energy Fuels 1992;6(5):581–5.
[10] Cookson DJ, Latten JL, Shaw IM, Smith BE. Property-composition relationships for diesel and kerosene fuels. Fuel 1985;64(4):509–19.
[11] Liu G, Wang L, Qu H, Shen H, Zhang X, Zhang S, et al. Artificial neural network approaches on composition–property relationships of jet fuels based on GC–MS. Fuel 2007;86(16):2551–9.
[12] Morris RE, Hammond MH, Cramer JA, Johnson KJ, Giordano BC, Kramer KE, et al. Rapid fuel quality surveillance through chemometric modeling of near-infrared spectra. Energy Fuels 2009;23(3):1610–8.
[13] Cramer JA, Hammond MH, Myers KM, Loegel TN, Morris RE. Novel data abstraction strategy utilizing gas chromatography–mass spectrometry data for fuel property modeling. Energy Fuels 2014;28(3):1781–91.
[14] Shi X, Li H, Song Z, Zhang X, Liu G. Quantitative composition-property relationship of aviation hydrocarbon fuel based on comprehensive two-dimensional gas chromatography with mass spectrometry and flame ionization detector. Fuel 2017;200:395–406.
[15] D1655-18b. Standard Specification for Aviation Turbine Fuels. West Conshohocken, PA: ASTM International; 2011.
[16] Vozka P, Mo H, Šimáček P, Kilaz G. Middle distillates hydrogen content via GC × GC-FID. Talanta 2018;186:140–6.
[17] Martens HK, Tøndel V, Tafintseva A, Kohler E, Plahte JO, Vik SW, et al. PLS-based multivariate metamodeling of dynamic systems. New Perspectives in Partial Least Squares and Related Methods. Springer; 2013. p. 3–30.
[18] Vincenzo V. Handbook of Partial Least Squares: Concepts, Methods and Applications. Berlin: New York: Springer; 2010.
[19] Haenlein M, Kaplan AM. A beginner's guide to partial least squares analysis. Understanding Stat 2004;3(4):283–97.
[20] Suykens JA, Van Gestel T, De Brabanter J. Least Squares Support Vector Machines. World Scientific; 2002.
[21] Bottou L. Large-scale machine learning with stochastic gradient descent. Proceedings of COMPSTAT'2010. Springer; 2010. p. 177–86.
[22] Ho CH, Lin CJ. Large-scale linear support vector regression. J Mach Learn Res 2012;13(Nov):3323–48.
[23] Hsieh CJ, Chang KW, Lin CJ, Keerthi SS, Sundararajan S. A dual coordinate descent method for large-scale linear SVM. Proceedings of the 25th International Conference on Machine learning. ACM; 2008.
[24] Garcia M, Rey C, Villar VP, Rodriguez JR. Excess volumes of (n-nonane n-undecane) between 288.15 and 308.15 K. J Chem Eng Data 1988;33(1):46.
[25] Zhang L, Guo Y, Xiao J, Gong X, Fang W. Density, refractive index, viscosity, and surface tension of binary mixtures of exo-tetrahydrodicyclopentadiene with somen-alkanes from (293.15 to 313.15) K. J Chem Eng Data 2011;56(11):4268.
[26] Liu H, Zhu L. Excess molar volumes and viscosities of binary systems of butylcyclohexane with n-alkanes (C7 to C14) at T = 293.15 K to 313.15 K. J Chem Eng Data 2014;59(2):369.
[27] Lobos J, Mozo I, Regúlez MF, González JA, García de la Fuente I, Cobos JC. Thermodynamics of mixtures containing a very strongly polar compound. 8. Liquid–liquid equilibria for N, N-dimethylacetamide + selected alkanes. J Chem Eng Data 2006;58(8):2339.
[28] Prak DJL, Prak PJL, Cowart JS, Trulove PC. Densities and viscosities at 293.15–373.15 K, speeds of sound and bulk modulus at 293.15–333.15 K, surface tensions, and flash points of binary mixtures of n-hexadecane and alkylbenzenes at 0.1 MPa. J Chem Eng Data 2017;62(5):1673.
[29] Rossini FD. Selected Values of Physical and Thermodynamic Properties of Hydrocarbons and Related Compounds: Comprising the Tables of the American Petroleum Institute Research Project 44, Extant as of December 31, 1952. Pittsburgh, PA: Carnegie Press; 1953.
[30] Findegg GH. Density and expansion coefficient of some liquid alkanes. Monatshefte Chem 101 (4), 1081.
[31] Forziati A, Glasgow A, Willingham C, Rossini F. Purification and properties of 29 paraffin, 4 alkylcyclopentane, 10-alkylcyclohexane, and 8 alkylbenzene hydrocarbons. J Res Natl Bur Stand 1946;36(2):129.
[32] Awwad AM, Pethrick RA. Isentropic compressibilities of hydrocarbons and their mixtures Mixtures of linear and branched-chain alkanes. J Chem Thermodyn 1984;16(2):131.
[33] Clarke L. Methyl ethyl isobutyl methane. J Am Chem Soc; 30 (7), 1144.
[34] Mears T, Fookson A, Pomerantz P, Rich E, Dussinger C, Howard F. Syntheses and properties of two olefins, six paraffins, and their intermediates. J Res Natl Bur Stand 1950;44(3):299.
[35] Calingaert G, Soroos H. The methyl nonanes. J Am Chem Soc, 635.
[36] Terres VE, Brinkmann L, Fischer D, Hullstrung D, Lorz W, Weisbrod G. Synthese und physikalische daten einiger isoparaffinreihen mit 11 bis 24C-atomen. Brenstoff-Chemie 1959;40:279.
[37] Johnson GC. Decenes formed from t-amyl alcohol and from 2-methyl-2-butene. Composition of the Hydrogenated Products. J Am Chem Soc 1947;69(1):146.
[38] Matilla A, Tardajos G, Aicart E. Thermodynamic mixing properties of (chlorobenzene an alkane). J Chem Thermodyn 1993;25(2):201.
[39] Kiryalov NP, Bagirov VY. Structure of karatavicin. Chem Nat Compd 1967;3(4):185.
[40] Fischer FG. The constitution of phytol. Justus Liebigs Annalen der Chemie, 464 (1), 82.
[41] Korosi G, Kovats ES. Density and surface tension of 83 organic liquids. J Chem Eng Data 1981;26(3):323.
[42] Fermeglia M, Torriano G. Density, viscosity, and refractive index for binary systems of n-C16 and four nonlinear alkanes at 298.15 K. J Chem Eng Data 1991;44(5):965.
[43] Forziati AF, Rossini FD. Physical properties of sixty API-NBS hydrocarbons. J Res Natl Bur Stand 1949;43(5):473.
[44] Jiang X, He G, Wu X, Guo Y, Fang W, Xu L. Density, viscosity, refractive index, and freezing point for binary mixtures of 1,1′-bicyclohexyl with alkylcyclohexane. J Chem Eng Data 2014;59(8):2499.
[45] Lozovoi AV, D'yakova MK, Stepantseva TG. Some physical constants of hydrocarbon mixtures: II. Zhurnal Obshchei Chim, 9, 540.
[46] Mears TW, Stanley CL, Compere EL, Howard FL. Synthesis, purification, and physical properties of seven twelve-carbon hydrocarbons. J Res Natl Bur Stand Section A 1963;67A(5):475.
[47] Ruzicka L, Veen AG. Höhere terpenverbindungen. XXXV. Über Die Konstitution Des Bisabolens. Justus Liebigs Annalen Chemie 1921;468(1):133.
[48] Camin DL, Forziati AF, Rossini FD. Physical properties of n-hexadecane, n-decylcyclopentane, n-decylcyclohexane, 1-hexadecene and n-decylbenzene. J Phys Chem 1954;58(5):440.
[49] Mann G. Cis- und trans-bicyclo-(3,2,0)-heptan. Z Chem 1966;6(3):106.
[50] Cope AC, Schmitz WR. Cyclic polyolefins. VII. Structure of the eight-membered cyclic dimer of chloroprene1. J Am Chem Soc 1950;72(7):3056.
[51] Camin DL, Rossini FD. Physical properties of fourteen API research hydrocarbons, C9 to C15. J Phys Chem 1955;59(11):1173.
[52] Weissenberger G, Henke R, Katschinka H. Zur kenntnis binärer flüssigkeitsgemische XX. Systeme mit substituierten hydronaphthalinen. Z Anorg Allg Chem 1926;153(1):33.
[53] Gudzinowicz BJ, Campbell RH, Adams JS. Specific heat measurements of complex saturated hydrocarbons. J Chem Eng Data 1963;8(2):201.
[54] Goodman IA, Wise PH. Dicyclic hydrocarbons. II. 2-alkylbicyclohexyls. J Am Chem Soc 1951;73(2):850.
[55] Lamneck JH, Wise PH. Dicyclic hydrocarbons. IX. Synthesis and physical properties

of the monomethyldiphenylmethanes and monomethyldicyclohexylmethanes. J Am Chem Soc 1954;76(4):1104.
[56] Ruzicka L, Meyer J, Mingazzini M. Höhere terpenverbindungen III. Über die naphtalinkohlenwasserstoffe cadalin und eudalin, Zwei aromatische grundkörper Der Sesquiterpenreihe. Helv Chim Acta 1922;5(3):345.
[57] Corson BB, Heintzelman WJ, Moe H, Rousseau CR. Reactions of styrene dimers. J Org Chem 1962;27(5):1636.
[58] Richard AJ, Fleming PB. The isothermal piezooptic coefficient and compressibility of some substituted benzenes and cyclic compounds. J Chem Thermodyn 1981;13(9):863.
[59] Birch SF, Dean RA, Fidler FA, Lowry RA. The preparation of the C10 monocyclic aromatic hydrocarbons. J Am Chem Soc 1949;71(4):1362.
[60] Good WD. The standard enthalpies of combustion and formation of n-butylbenzene, the dimethylethylbenzenes, and the tetramethylbenzenes in the condensed state. J Chem Thermodyn 1975;7(1):49.
[61] Luning Prak DJ, Luning Prak PJ, Cowart JS, Trulove PC. Densities and Viscosities at 293.15–373.15 K, speeds of sound and bulk moduli at 293.15–333.15 K, surface tensions, and flash points of binary mixtures of n-hexadecane and alkylbenzenes at 0.1 MPa. J Chem Eng Data 2017;62(5):1673–88.
[62] Good W. The enthalpies of combustion and formation of indan and seven alkylindans. J Chem Thermodyn 1971;3(5):711.
[63] Entel J, Ruof CH, Howard HC. Preparation and properties of some methylated indans. Anal Chem 1953;25(9):1303.
[64] Wood TF, Easter WM, Carpenter MS, Angiolini J. Polycyclic musks. I. Acyl- and dinitropolyalkyltetralin derivatives. J Org Chem 1963;28(9):2248.
[65] Bogert MT, Davidson D, Apfelbaum PM. The synthesis of condensed polynuclear hydrocarbons by the cyclodehydration of aromatic alcohols. II. The synthesis of ionenes. J Am Chem Soc 1934;56(4):959.
[66] Boedtker MME, Rambech O. Recherches sur quelques derives du tetraet du decahydronaphthalene. Bulletin de la Societe Chimique de France, 35, 631.
[67] Weissenberger G, Henke R, Katschinka H. Zur kenntnis inärer flüssigkeitsgemische XX. systeme mit substituierten hydronaphthalinen. Z Anorg Allg Chem 1926;153(1):33.
[68] Perkin WH. On magnetic rotatory power, especially of aromatic compounds. J Chem Soc Trans 1896;69:1025.
[69] Arrowsmith GB, Jeffery GH, Vogel AI. 369. Physical properties and chemical constitution. Part XLI. Naphthalene compounds. J Chem Soc 1965;2072.
[70] Ruzicka L, Veen AGV. Höhere terpenverbindungen. XL. zur kenntnis der konstitution des elemols. Justus Liebigs Ann Chem 1929;476(1):70.
[71] Dimitrov C, Popova Z. Dehydrocyclization of α-amylnaphthalene on silica-alumina catalyst. J Catal 1967;9(1):1.